958 *Macromolecules* **2011**, *44*, 958–965
DOI: 10.1021/ma102195y

Macromolecules
ARTICLE

Hierarchical Nanostructures in Semifluorinated Norbornene Block Copolymers

B. Pulamagatta,*,† S. Pankaj,‡ M. Beiner,*,‡,§ and W. H. Binder†

†*Chair of Macromolecular Chemistry, Institute of Chemistry, Division of Technical and Macromolecular Chemistry, Faculty of Natural Sciences II, Martin-Luther-University Halle-Wittenberg, Von-Danckelmann-Platz 4, D-06120 Halle, Germany,* ‡*Faculty of Natural Sciences II, Martin-Luther-University Halle-Wittenberg, D-06099 Halle, Germany, and* §*Fraunhofer Institute for Mechanics of Materials, Walter-Hülse-Str. 1, D-06120 Halle, Germany*

Received September 24, 2010; Revised Manuscript Received December 31, 2010

ABSTRACT: Structure and dynamics of two microphase-separated norbornene block copolymers containing one comb-like component are investigated by X-ray scattering, relaxation spectroscopy as well as differential scanning calorimetry. It is shown that two self-assembling processes on different length scales coexist for these copolymers leading to hierarchically structured systems. Microphase separation of both block copolymer components appears on a scale of 20−25 nm while norbornene main and long semifluorinated side chains of the comb-like block nanophase separate within their domains on a scale of about 3 nm. This hierarchical structure is accompanied by a complex relaxation behavior which is characterized by two glass transitions. The glass temperature of the block with long bulky side chains is expectedly lower due to internal plasticization. An additional relaxation process showing typical features of a dynamic glass transition is related to an independent dynamics in small nanodomains formed by long aggregated side chains similar to the findings for many other comb-like polymers. Indications for the disappearance of the nanophase separation of main and semifluorinated side chains at high temperatures are discussed.

1. Introduction

Self-assembled polymers are an important class of materials for various applications requiring well-defined structures with typical dimensions below 50 nm.[1] Archetype examples are diblock copolymers containing two incompatible components which aggregate in domains with typical dimensions comparable to the radius of gyration of the individual blocks (typical values are 5−30 nm). Depending on the volume fraction of both blocks, systems with different phase morphologies like lamellar, cylindrical, spherical, or gyroidal structures will form. Phase behavior and phase separation processes in block copolymers are well understood and thermodynamic models to describe the situation are established.[2,3]

In the recent years, there has been an increasing interest in systems with more complicated phase structure and in particular in self-assembled polymers with a hierarchical structure incorporating different well-defined length scales.[4−6] One approach to design such systems is a combination of classical microphase separation effects in block copolymers with self-assembling tendencies which exist in comb-like polymers leading to lamellar structures with typical dimensions in the 1−3 nm range.[7−10] Lamellar packing of main and side chains is well-known for side chain polymers containing stiff units at the end of the side chains, which can appear in a liquid crystalline state[7,8] or systems with long alkyl side chains where the methylene units far away from the backbone can crystallize.[9,10] However, nanophase separation of incompatible main and side chain parts is also indicated for comb-like polymers containing shorter, noncrystallizable alkyl groups in the side chain.[11−13] The alkyl groups in these systems also aggregate to form small alkyl nanodomains surrounded by main chains. Nanophase separation in fully amorphous side chain polymers is indicated by (i) relatively broad peaks in X-ray diffraction pattern in the range $2 \leq q \leq 6$ nm^{-1} (often called prepeaks in the recent literature) corresponding to an equivalent Bragg spacing of 1−3 nm and (ii) an independent polyethylene-like dynamics within the alkyl nanodomains, seen as α_{PE} process in relaxation data at low temperatures, which shows typical features characteristic for other cooperative relaxation processes.[12,14] Both effects are observed for various series of side chain polymers containing long alkyl groups. They are basically independent of microstructure and softening behavior of the main chain. Hence it was concluded that nanophase separation is a general phenomenon in such systems.[14,15] Temperature dependent measurements on selected series show that the behavior is not changing at high temperatures, i.e., that the underlying structure is relatively unaffected by temperature changes.[13] A theoretical description of nanophase separation phenomena, however, is still not available, although first approaches have been developed and applied to systems where the side chains are noncovalently bonded to the backbone[16] or weakly grafted systems.[17]

Nanophase separation effects due to demixing of incompatible main and side chains are also expected and found in cases where the side chains are no alkyl groups. Lamellar structures with typical periodicities in the 1−3 nm range are reported in particular for polymers with fluorinated or semifluorinated side chains[18−20] as well as long poly(ethylene oxide) sequences as side chains.[21] From the structural point of view the situation at room temperature seems to be similar to that in systems with alkyl side chains but it is unclear (i) whether or not there is also an independent dynamics within the side chain domains in these cases and (ii) to what extent changes in the nanophase separation behavior appear with temperature. One aim of this paper is to answer such questions based on a systematic study of two norbornene diblock copolymers containing a comb-like semifluorinated component. The morphology of these hierarchically structured systems is studied by scattering experiments and their

*Corresponding author.

 Published on Web 01/25/2011

relaxation behavior is investigated by different relaxation spectroscopy methods as well as calorimetry in order to understand structure−property relationships. Temperature-dependent changes in the structure observed above 30 °C might be interesting for a better understanding of nanophase separation phenomena in the future.

2. Experimental Section

2.1. Methods. *X-ray Scattering Experiment*. X-ray scattering measurements were performed on a small angle instrument assembled by JJ X-rays based on a 2D Hi-Star detector by Bruker and a Rigaku rotating anode with focusing optics. Cu Kα radiation with a wavelength $\lambda = 1.54$ Å was used for all measurements. The scattering angles θ of the instrument were calibrated using silver behanate as a reference material. For temperature-dependent measurements a Linkam hot stage was used with equilibration time of 15 min. Small angle X-ray scattering (SAXS) experiments were performed at scattering vectors $q = 4\pi(\sin\theta)/\lambda$ in the range $0.009\ \text{Å}^{-1} \le q \le 0.15\ \text{Å}^{-1}$ and medium angle X-ray scattering (MAXS) data were recorded in the range $0.15\ \text{Å}^{-1} \le q \le 0.60\ \text{Å}^{-1}$.

Dynamic Mechanical Analysis. Dynamic shear modulus $G^* = G' + iG''$ was measured using an Anton Paar MCR501 instrument. A control strain of 0.015% was used. Isotherms were measured at angular frequencies $\omega = 2\pi f$ in the range $0.1\ \text{rad/s} \le \omega \le 100\ \text{rad/s}$ with five points per decade. Equilibration time at each temperature was 180 s with a temperature step of 4 K. For the temperature scans, a rate of 1 K/min was used at a constant angular frequency of 10 rad/s with point density of 2 points/min. All the measurements were performed in a controlled nitrogen gas atmosphere.

Differential Scanning Calorimetry. A Perkin-Elmer Diamond DSC was used for measurements with heating rates of $dT/dt = 10$ K/min. Samples with a mass of about 5 mg were encapsulated in standard 10 μL pans.

Dielectric Spectroscopy. The dielectric function $\varepsilon^*(\omega) = \varepsilon'(\omega) - i\varepsilon''(\omega)$ was measured using a Novocontrol Alpha analyzer in the frequency range $10^{-1}\ \text{Hz} \le f \le 10^5\ \text{Hz}$. Measurements were performed on films with 25 μm thickness pressed between gold plated brass electrodes with a diameter of 20 mm using kapton spacers. Isotherms were measured at temperatures between −120 and +140 °C with a temperature step of 5 K.

2.2. Synthesis of the Samples. *Materials*. Grubbs first generation catalyst was obtained from Sigma-Aldrich. Dichloromethane (CH_2Cl_2) was freshly distilled over CaH_2 and degassed with argon prior to use. The other solvents like petrolether and ethyl acetate were used after distillation. All other reagents were purchased from Sigma-Aldrich (Germany) and were used without further purification.

Sample Characterization. The chemical characterization of synthesized compounds was done via ^{1}H NMR measurements performed on a Varian Gemini 200 or 400 MHz FT-NMR spectrometer using MestRec (4.9.9.9) for the data evaluation. Molecular weight distributions and polymerization kinetics were determined by GPC measurements done on a Viscotek VE2001 system using polystyrene standards for conventional external calibration with Viscotek VE3580 refractive index detector.

Monomer Synthesis. *endo*,*exo*-Bicyclo[2,2,1]-hept-5-ene-2,3-dicarboxylic acid dimethylester (monomer **A**) was prepared according to the procedure from ref 22, *endo*,*exo*-bicyclo[2,2,1]-hept-5-ene-2,3-dicarboxylic acid bis(3,3,4,4,5,5,6,6,7,7,8,8,8-tridecafluorooctyl) ester (monomer **C**) was prepared according to modified procedure from above-mentioned ref 22 (described below). A dry round-bottom flask equipped with magnetic stir bar was flushed with argon and charged with *endo*,*exo*-bicyclo-[2,2,1]-hept-5-ene-2,3-dicarboxylic acid (2.5 g, 13.73 mmol) and excess thionyl chloride ($SOCl_2$) (8.23 mL, 0.114 mol). The mixture was refluxed for 4 h at 90 °C and subsequently excess of thionyl chloride was removed under reduced pressure to obtain *endo*,*exo*-bicyclo[2,2,1]-hept-5-ene-2,3-dicarboxylic acid chloride. Further 1*H*,1*H*,2*H*,2*H*-perfluoro-1-octanol (15.78 mL, 34.3 mmol) and pyridine (3.68 mL, 50.2 mmol) were dissolved in 40 mL of dry CH_2Cl_2. Under ice cooling *endo*,*exo*[2.2.1] bicyclo-2-ene-5,6-dicarboxylic acid chloride (2.42 g, 11.42 mmol) was dropped into the reaction mixture and stirred overnight at room temperature. The reaction mixture was filtered to remove the pyridinium salt and extracted with CH_2Cl_2. The organic layer was extracted with 2 N HCl solution, saturated sodium bicarbonate and dried with sodium sulfate. The solvent was removed under reduced pressure. Finally, the product was purified using column chromatography with petrolether/ethyl acetate (10:1) as the solvent mixture to yield 6.96 g (70%) of monomer **C** as a white solid.

Scheme 1. Structure of the Investigated A_m-*b*-C_n Block Copolymers

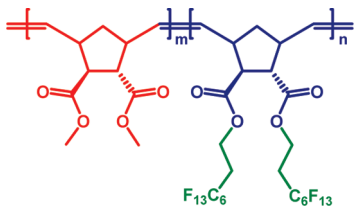

^{1}H NMR (δ ppm, $CDCl_3$, 400 MHz): 6.27 (dd, J= 5.59, 3.12 Hz, 1H), 6.06 (dd, J= 5.61, 2.81 Hz, 1H), 4.36 (td, J_{H-F}=30.16, 6.35 Hz, 4H), 3.40−3.20 (m, 2H), 3.17−3.06 (m, 1H), 2.66 (dd, J= 4.57, 1.65 Hz, 1H), 2.44 (tq, J^1_{FC}=19.41, J=6.32 Hz, 4H), 1.64−1.41 (m, 2H).

Polymer Synthesis. The homopolymer $\mathbf{A}_{200}$ was synthesized via ROMP using Grubbs first generation catalyst according to the procedures developed previously in our laboratory.[22,23] The substituted norbornene block copolymers, $\mathbf{A}_m$-*b*-$\mathbf{C}_n$, in which one block (block **A**) containing two methyl ester groups ($COOCH_3$) per repeating unit and the other (block **C**) containing two fluorinated alkyl ester ($COOCH_2CH_2(CF_2)_5CF_3$) side chains were synthesized by the sequential addition of respective monomers using Grubbs first generation catalyst. The general synthetic procedure of block copolymer $\mathbf{A}_m$-*b*-$\mathbf{C}_n$ is described below, for $\mathbf{A}_{50}$-*b*-$\mathbf{C}_{13}$ as an example. Monomer **A** (240.2 mg, 1.2 mmol) in 2 mL of CH_2Cl_2 was added to the Grubbs first-generation catalyst, $[RuCl_2(PCy_3)_2(CHPh)]$ (18.8 mg, 0.022 mmol) dissolved in 2 mL of CH_2Cl_2 in a heated and argon-flushed glass vial equipped with a magnetic stir bar. The polymerization was carried out at room temperature for 2 h until all of monomer **A** was consumed, as checked by TLC. Monomer **C** (259.8 mg, 0.3 mmol) as a solution in 2 mL of CH_2Cl_2 was then added to the above reaction mixture and stirred for 7 h at room temperature until all of the monomer **C** was consumed, as checked by TLC. The polymerization was quenched by adding cold ethyl vinyl ether. The produced polymer was isolated by precipitating in to cold methanol. Finally the product was dried under high vacuum overnight to yield 485 mg (97%) of $\mathbf{A}_{50}$-*b*-$\mathbf{C}_{13}$. The other block copolymer $\mathbf{A}_{50}$-*b*-$\mathbf{C}_8$ with different block composition was synthesized using the above stated procedure but adopting the different monomer/initiator ratio. The general structure of $\mathbf{A}_m$-*b*-$\mathbf{C}_n$ is given in Scheme 1.

Before establishing the above stated polymerization procedure, the increase in molecular weight (M_n) with the polymerization time was monitored by GPC. Monomer **A** was first polymerized for 2 h to obtain living polymer $\mathbf{A}_{50}$ chain with molecular weight ($M_{n(GPC)}$ = 8.4 kg/mol) which was comparable to the calculated molecular weight ($M_{n(CAL)}$) with low polydispersity index (PDI = 1.17). Furthermore, monomer **C** was added to the above reaction mixture. After 4 h of adding monomer **C** the M_n was increased to 16.4 kg/mol according to GPC measurements suggesting addition of ∼10 units of monomer **C** onto the polymer $\mathbf{A}_{50}$ chain and confirming the crossover reaction. However further proceeding with the reaction no remarkable increase in the molecular weight was noticed, instead there was an increase in the PDI value and also precipitation occurred.

Table 1. Characterization of the Polymers

sample	$M_{n(cal)}$ (kg/mol)	$M_{n(GPC)}$ (kg/mol)	PDI	$T_{g,A}$ (°C)	$T_{g,C}$ (°C)
$\mathbf{A}_{200}$	42.0	40.0	1.17	72	
$\mathbf{A}_{50}$-*b*-$\mathbf{C}_{13}$	21.9	16.4	1.20	70	25
$\mathbf{A}_{50}$-*b*-$\mathbf{C}_{8}$	17.5	13.0	1.20	67	22

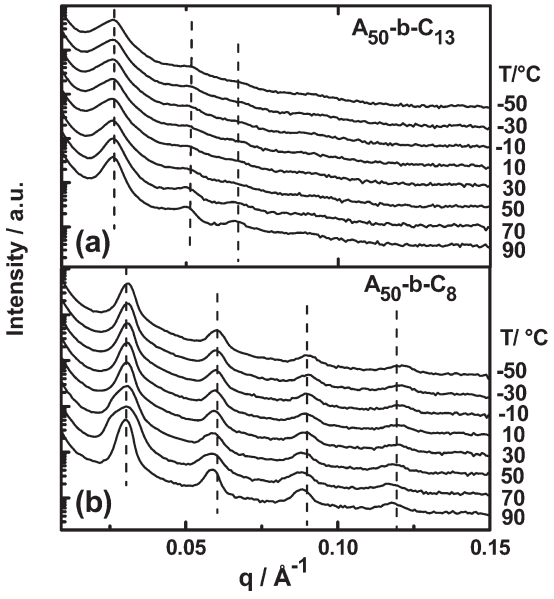

Figure 1. Small angle X-ray scattering curves for (a) $\mathbf{A}_{50}$-*b*-$\mathbf{C}_{13}$ and (b) $\mathbf{A}_{50}$-*b*-$\mathbf{C}_{8}$ measured at different temperatures. The data sets are vertically shifted for the sake of clarity.

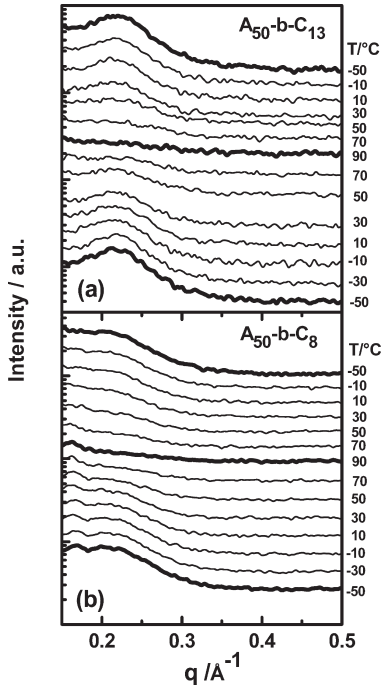

Figure 2. X-ray scattering curve in the mediate q range (0.15 $Å^{-1} \leq q \leq$ 0.50 $Å^{-1}$) for (a) $\mathbf{A}_{50}$-*b*-$\mathbf{C}_{13}$ and (b) $\mathbf{A}_{50}$-*b*-$\mathbf{C}_{8}$. Heating scans (from −50 to +90 °C) and subsequent cooling (+90 °C to −50 °C) scans are shown from the top to the bottom. The curves are vertically shifted.

An analysis of integral values in ^{1}H NMR spectra suggested that only 13−16 units of **C** had added onto the polymer **A** chain (see Supporting Information for GPC and NMR results). The precipitation indicates that the limited solubility of the block copolymer is responsible for stopping the polymerization. Thus, a maximum of 13−16 repeating units of monomer **C** could be polymerized onto the polymer **A** chain irrespective of the chain length of **A**. Two block copolymers were synthesized keeping the block **A** length constant to 50 units. The length of the **C** block is varied. The **C** block of sample $\mathbf{A}_{50}$-*b*-$\mathbf{C}_{8}$ contains 8 **C** units, while that of the $\mathbf{A}_{50}$-*b*-$\mathbf{C}_{13}$ contains 13−16 **C** units. Further information about the microstructure of the synthesized polymers is summarized in Table 1.[24]

3. Results

Microphase separation and morphology of the synthesized $\mathbf{A}_m$-*b*-$\mathbf{C}_n$ block copolymers are analyzed by small-angle X-ray scattering (SAXS) experiments at scattering vectors in the range of 0.009 $Å^{-1} \leq q \leq 0.15$ $Å^{-1}$. Figure 1 shows SAXS pattern for the block copolymers $\mathbf{A}_{50}$-*b*-$\mathbf{C}_{13}$ and $\mathbf{A}_{50}$-*b*-$\mathbf{C}_{8}$ measured at temperatures between −50 and +90 °C. The presence of prominent higher order reflections up to the fourth order for both samples is a clear evidence for the existence of well ordered periodic structures formed due to microphase separation of **A** and **C** blocks. In case of $\mathbf{A}_{50}$-*b*-$\mathbf{C}_{13}$, the first order peak appears at $q_1 = 0.026$ $Å^{-1}$ corresponding to a long period of $d_1 = 24$ nm according to Bragg's law ($d_1 = 2\pi/q_1$). The relative peak positions of the higher order peaks with q_1 are in the ratio of $1:\sqrt{4}:\sqrt{7}:\sqrt{9}$ suggesting a hexagonally ordered cylindrical structure. In case of the $\mathbf{A}_{50}$-*b*-$\mathbf{C}_{8}$ sample a narrow first order peak appears at $q_1 = 0.030$ $Å^{-1}$ related to a long period of $d_1 = 21$ nm. The higher order peaks are equidistantly spaced relative to q_1 (1:2:3:4) confirming a lamellar morphology of this sample. The scattering pattern of both samples does not show a significant change with temperature; i.e., the block copolymer morphology is preserved in the investigated temperature range. Both block copolymers are obviously strongly segregated at temperatures below 90 °C and far away from any order-to-disorder transition (ODT). The observed change from cylindrical to lamellar morphology upon decreasing the length of block **C** from 13 to 8 monomeric units indicates that the **C** phase forms the matrix in block copolymer $\mathbf{A}_{50}$-*b*-$\mathbf{C}_{13}$, i.e., that cylindrical **A** domains are surrounded by a continuous **C** phase in this case. Although block **C** has a lower degree of polymerization compared to block **A**, the volume fraction of the **C** phase seems to be large due to the bulkiness of the semifluorinated alkyl side chains.[24]

Nanophase separation of the semifluorinated side chains from the norbornene main chains in the domains containing block **C** is evidenced by X-ray scattering data in the intermediate q range (0.15 $Å^{-1} \leq q \leq 0.50$ $Å^{-1}$). Figure 2 shows corresponding scattering pattern for $\mathbf{A}_{50}$-*b*-$\mathbf{C}_{13}$ and $\mathbf{A}_{50}$-*b*-$\mathbf{C}_{8}$ respectively. Heating (−50 °C → +90 °C) and cooling (+90 °C → −50 °C) scans are performed in order to check the reversibility of temperature dependent changes. A middle angle X-ray scattering (MAXS) peak at $q_{nps} = 0.22$ $Å^{-1}$ is seen at temperatures below 70 °C for both the samples. This maximum position corresponds to equivalent Bragg spacings d_{nps} of about 2.9 nm. Broad peaks in this q range are commonly observed for amorphous comb-like polymers containing long alkyl side chains due to nanophase separation of main and side chain parts.[13−15,25] For the investigated block copolymer systems the peak in the MAXS range indicates demixing of norbornene backbone and semifluorinated alkyl side chains of block **C**. Note that the MAXS peaks are extremely broad indicating that there is no pronounced long-range order. Interestingly, the MAXS peak gradually vanishes upon heating between 30 and 90 °C and reappears upon cooling in the same temperature range (Figure 2). This observation suggests that the nanophase separation, i.e. the demixing of semifluorinated alkyl side chains from the main polymer chains, occurs only below this temperature interval while both subunits are mixed in the **C** phase

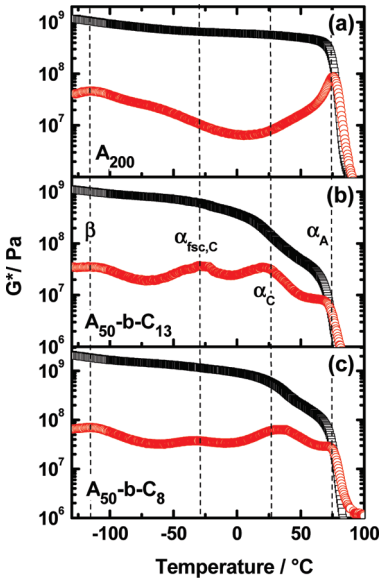

Figure 3. Shear storage G′ (□) and shear loss modulus G″ (○) as function of temperature for (a) $\mathbf{A}_{200}$, (b) $\mathbf{A}_{50}$-*b*-$\mathbf{C}_{13}$, and (c) $\mathbf{A}_{50}$-*b*-$\mathbf{C}_{8}$. The vertical dotted lines indicate the temperature positions of the different relaxation processes (α_A, α_C, $\alpha_{fsc,C}$, β).

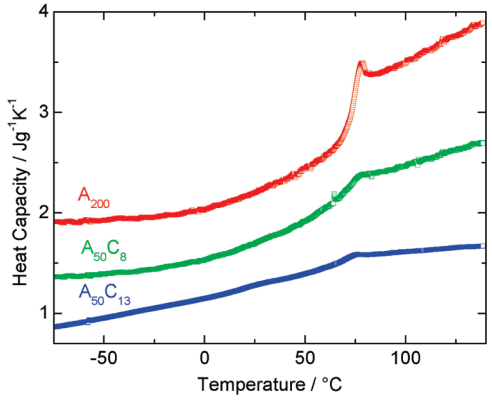

Figure 4. DSC heating scans measured with a rate of $dT/dt = +10$ K/min for homopolymer $\mathbf{A}_{200}$ and both block copolymers $\mathbf{A}_{50}$-*b*-$\mathbf{C}_{8}$ as well as $\mathbf{A}_{50}$-*b*-$\mathbf{C}_{13}$. The heat capacity curves for $\mathbf{A}_{50}$-*b*-$\mathbf{C}_{8}$ and $\mathbf{A}_{200}$ are vertically shifted by 0.5 and 1 J/gK, respectively.

at higher temperatures. Similar behavior has not been reported to our knowledge for nanophase-separated polymers containing alkyl side chains which are covalently bonded to different backbones.

Dynamic shear modulus $G^*(T) = G'(T) + iG''(T)$ data, with G' being the storage and G'' the loss modulus, for homopolymer $\mathbf{A}_{200}$ as well as the two block copolymers $\mathbf{A}_{50}$-*b*-$\mathbf{C}_{13}$ and $\mathbf{A}_{50}$-*b*-$\mathbf{C}_{8}$ are shown in Figure 3. Two independent relaxation processes at around −115 and +77 °C are observed in 10 rad/s isochrones for homopolymer $\mathbf{A}_{200}$ (Figure 3a). The low temperature process at −115 °C showing an Arrhenius-like temperature dependence (see below) corresponds to a local mode β, whereas the process at 75 °C is the segmental relaxation α_A caused by co-operative motions of complete monomeric units leading to a softening of the entire system. The glass temperature $T_{g,A}$ taken from DSC scans performed with a heating rate of 10 K/min (Figure 4, Table 1) is comparable to the relaxation temperature for the α_A process, $T_{\alpha,A}$, as obtained from shear measurements with an angular frequency ω of 10 rad/s. The β and α_A processes, which are already seen for the neat homopolymer $\mathbf{A}_{200}$, do also appear in the microphase-separated block copolymers $\mathbf{A}_{50}$-*b*-$\mathbf{C}_{13}$ and $\mathbf{A}_{50}$-*b*-$\mathbf{C}_{8}$ at −120 °C and at 77 °C (Figure 3, parts b and c), i.e., the relaxation processes of the $\mathbf{A}_{50}$ block are expectedly quite comparable to that for the $\mathbf{A}_{200}$ homopolymer. Additional relaxation processes in the shear curves for the two block copolymers at −29 and +22 °C originate obviously from block **C**. DSC measurements on $\mathbf{A}_m$-*b*-$\mathbf{C}_n$ block copolymers give glass temperatures for block **C** in the range $T_{g,C} = 23 \pm 2$ °C (Figure 4, Table 1). Hence, the relaxation process occurring at $T_{\alpha,C} = 22$ °C can be assigned to the segmental relaxation α_C of block **C**. The glass temperature of block **C** is reduced in comparison to that of block **A** due to internal plasticization of the main chains by the highly flexible side chains as discussed by Heijboer for poly(*n*-alkyl methacrylates).[26] The T_g shift in norbornene with semifluorinated side chains, however, seems to be smaller compared to that for PnAMAs with similar side chain length. The T_g difference between atactic PMMA and PnOMA is about 120 K[12] while the T_g difference between the **A** and **C** components of our block copolymers with similar side chain lengths is only 55 K. The additional relaxation process $\alpha_{fsc,C}$ at −29 °C is probably related to co-operative motions within small self-assembled side chain domains occurring due to nanophase separation within phase **C** at low temperatures. The $\alpha_{fsc,C}$ process can be understood as an additional indication for the presence of nanoscopic domains formed by segregation of long semifluorinated side chains. Unfortunately, it was not possible to prove this interpretation based on relaxation data for a neat **C** homopolymer since the synthesis of such systems is not feasible yet due to solubility limitations. Note that it remains open here whether the β relaxation appearing in both block copolymers near −115 °C is only caused by localized motions in the **A** phase. It may also incorporate localized motions of similar nature in the **C** phase which are strongly superimposed with contributions from the **A** phase ($\beta = \beta_A + \beta_C$). A clarification of the nature of the underlying motions requires studies with more selective methods like solid state NMR spectroscopy.

Considering the microstructure of our $\mathbf{A}_m$-*b*-$\mathbf{C}_n$ block copolymers (Scheme 1) dielectric spectroscopy should be also a suitable method to study the relaxation behavior since the polar carboxyl groups (−C(=O)O−) in both blocks act as dielectrically active centers. An additional dipole arises in the side chains of the block **C** originating from the uncompensated end fluorine atom.[27] Hence dielectric measurements in the frequency range from 10^{-1} to 10^5 Hz have been performed at temperatures between −140 and +140 °C.

The discussion here will be focused on results obtained at low temperatures (−140 °C ≤ T ≤ +10 °C) showing two secondary relaxations (β and γ) as well as the $\alpha_{fsc,C}$ process (Figure 5). The dielectric loss curves $\varepsilon''(\omega)$ measured at temperatures above 10 °C are dominated by strong conductivity contributions ($\varepsilon'' \sim \sigma/\varepsilon_0\omega$). Hence the α_A, α_C, and $\alpha_{fsc,C}$ processes are practically hidden in these isotherms or only seen as a weak shoulder which cannot be seriously evaluated. The low temperature isotherms $\varepsilon''(\omega)$ for the homopolymer $\mathbf{A}_{200}$ show a very broad and weak relaxation peak which shifts expectedly to higher frequencies if the temperature increases (Figure 5a). Its peak width decreases with increasing temperature. On the basis of a comparison of the peak maxima positions with those taken from shear curves (Figure 6) as well as a closer inspection of peak shape and width as a function of temperature one can conclude that this peak contains contributions from two secondary relaxation processes, β and γ, indicating the appearance of two different types of localized motions in glassy $\mathbf{A}_{200}$. Unfortunately, it is not possible to deconvolute the contributions of both relaxation processes in this case. Thus, only the maxima of the β process appearing at the low frequency end of the broad peak will be incorporated in the further discussion. The maxima positions are taken directly from the ε'' isotherms as indicated by ticks in Figure 5a.

Dielectric loss isotherms for the block copolymer $\mathbf{A}_{50}$-*b*-$\mathbf{C}_{13}$ measured at comparable temperatures are given in Figure 5c.

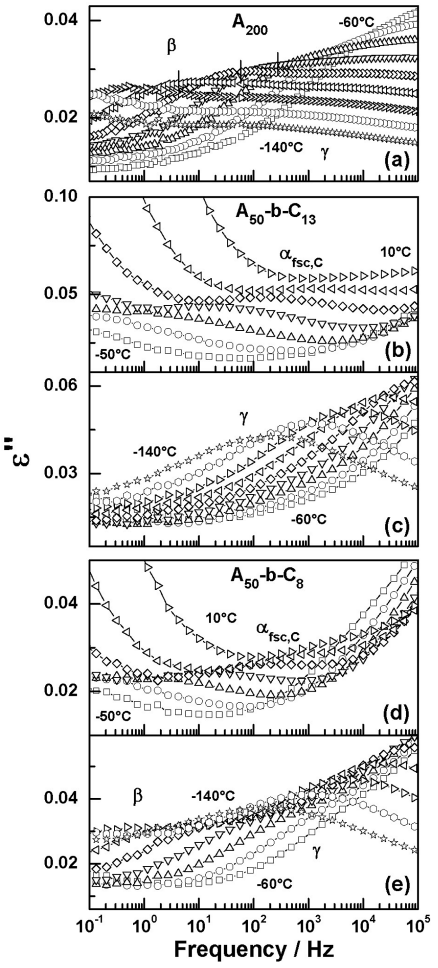

Figure 5. Dielectric loss ε'' isotherms for (a) $\mathbf{A}_{200}$, (b & c) $\mathbf{A}_{50}$-*b*-$\mathbf{C}_{13}$, and (d & e) $\mathbf{A}_{50}$-*b*-$\mathbf{C}_{8}$. The temperature limits are labeled in the individual plots. The temperature step between the shown isotherms is always 10K.

The results show clearly that the shape of the peak in $\varepsilon''(\omega)$ has changed. The peak maximum appears now at the high frequency end of the broad peak and β contributions dominating in the isotherms for the $\mathbf{A}_{200}$ homopolymer seem to be strongly suppressed. The γ process dominates obviously in case of this block copolymer. Similar behavior with slightly stronger contributions of the β process is observed for the $\mathbf{A}_{50}$-*b*-$\mathbf{C}_8$ block copolymer (Figure 5e). The experiments show commonly that the γ relaxation process is amplified and the β relaxation is suppressed if semifluorinated side chains (**C** units) are incorporated in the system. This is interesting since the main chains of both blocks, **A** and **C**, are identical. The only difference between both components is the long, semifluorinated side chain carrying only a small dipole but contributing significantly to the volume of the **C** block. Such a significant difference between the dielectric spectra for $\mathbf{A}_{200}$ and both block copolymers is somehow unexpected since the number of monomeric units (and (−C(=O)O−) groups) in the **C** block is small as compared to that in the **A** block. However, one has to take into account that the detected dielectric signals are tiny and that the long semifluorinated alkyl side chains of the **C** block possess an additional dipole. The results seem to indicate that the bulky side chains either amplify the γ relaxation which exists also for **A** polymers without side chains or that an extra relaxation process $\gamma_{\mathbf{C}}$ appears in the **C** block at a very similar frequency−temperature position. The latter case seems to be unlikely but cannot be completely excluded.

The $\alpha_{fsc,\mathbf{C}}$ process of the **C** block is observed in the dielectric data at intermediate temperatures ($-50\ °C \leq T \leq 10\ °C$, Figure 5, parts b and d) in accordance with shear data for both block copolymers. Like discussed above this relaxation process should reflect motions within nanodomains formed by aggregated side chains of the **C** block. The small dielectric relaxation strength of the $\alpha_{fsc,\mathbf{C}}$ process and the temperature dependence of the relaxation frequency $\omega_{\alpha sc}$ which corresponds to that obtained for the $\alpha_{fsc,\mathbf{C}}$ process in shear data (Figure 6) fit to this interpretation. Unfortunately it is impossible to get quantitative information about the temperature dependence of relaxation strength and shape for the $\alpha_{fsc,\mathbf{C}}$ peak in our systems since it is located in the valley between the $\alpha_{\mathbf{C}}$ and β/γ peaks. In this frequency range various relaxation processes do superimpose. Clear is that the $\alpha_{fsc,\mathbf{C}}$ peak moves out of the frequency window of our measurements above 10 °C significantly below the temperature where the MAXS peak disappears in the diffraction pattern as shown in Figure 2. Thus, it is impossible to study the influence of structural changes above 30 °C on the $\alpha_{fsc,\mathbf{C}}$ relaxation dynamics directly. Note that a relaxation process of semifluorinated side chains in practically the same frequency−temperature range has been reported for block copolymers where such side chains with different lengths (C_4F_9, C_8F_{17}) have been attached to a polybutadiene backbone. For the longer side chain, this peak has a bimodal relaxation time distribution in this case which was interpreted as an indication for the anisotropy of the underlying motions.[26]

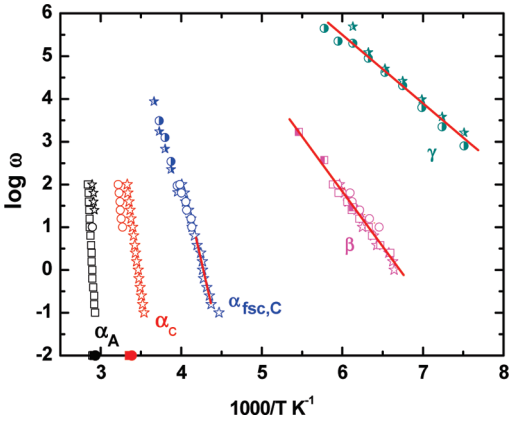

Figure 6. Arrhenius plot for the $\mathbf{A}_{200}$ homopolymer (squares) and the block copolymers $\mathbf{A}_{50}$-*b*-$\mathbf{C}_{13}$ (stars) and $\mathbf{A}_{50}$-*b*-$\mathbf{C}_8$ (circles) obtained from peak maxima positions of shear isochrones (open symbols) and dielectric isotherms (half filled symbols). The five different relaxation processes ($\alpha_{\mathbf{A}}$, $\alpha_{\mathbf{C}}$, α_{FS}, β, γ) appearing in these samples are labeled. DSC glass temperatures from scans with a heating rate of 10 K/min (solid symbols) are shown for comparison. Straight lines indicate Arrhenius fits as discussed in the main text.

An Arrhenius plot summarizing the information about the temperature dependence of all five relaxation processes ($\alpha_{\mathbf{A}}$, $\alpha_{\mathbf{C}}$, $\alpha_{fsc,\mathbf{C}}$, β and γ) in our $\mathbf{A}_n$-*b*-$\mathbf{C}_m$ block copolymers is given in Figure 6. The $\alpha_{\mathbf{C}}$ and $\alpha_{fsc,\mathbf{C}}$ relaxations appear only in the **C** block and have not been found for the $\mathbf{A}_{200}$ homopolymer. The results from shear and dielectric spectroscopy do basically coincide. Small shifts of the order of half a decade between the loss maxima positions in dielectric and shear curves might be due to the fact that both methods measure different susceptibilities and accordingly also different fluctuations.[28] Note that the frequency temperature position of all relaxation processes is nearly identical if $\mathbf{A}_{50}$-*b*-$\mathbf{C}_{13}$ and $\mathbf{A}_{50}$-*b*-$\mathbf{C}_8$ samples are compared, i.e. the dynamics is practically independent of the block copolymer morphology. The segmental dynamics ($\alpha_{\mathbf{A}}$) of the **A** block in both microphase-separated block copolymers corresponds to that in homopolymer $\mathbf{A}_{200}$ containing the same monomeric units but having higher molecular weight. The segmental relaxation $\alpha_{\mathbf{C}}$ of the **C** block with long semifluorinated side chains appears at significantly lower temperature. The glass temperatures from DSC scans with

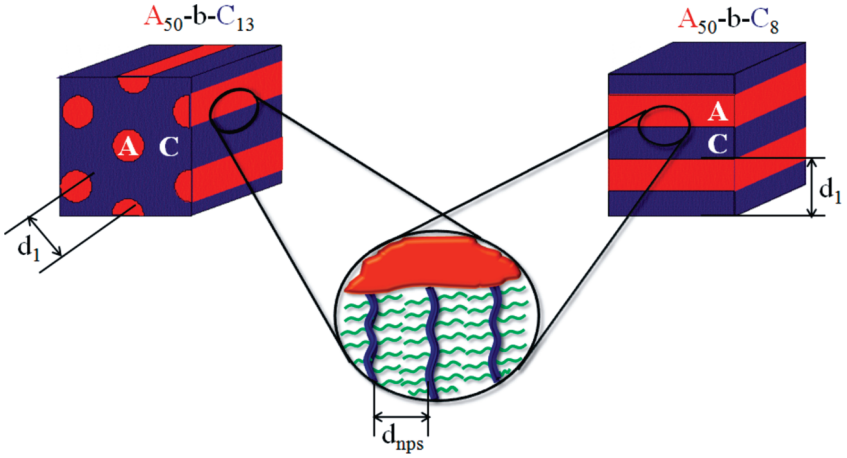

Figure 7. Scheme of the structural situation in the block copolymers $\mathbf{A}_{50}$-*b*-$\mathbf{C}_{13}$ (left) and $\mathbf{A}_{50}$-*b*-$\mathbf{C}_8$ (right) with cylindrical and lamellar morphology, respectively. The zoom in the middle shows the situation at the interface and the internal structure of the nanophase separated phase **C**.

a heating rate of 10 K/min are comparable with estimates determined based on an extrapolation of $\alpha_{\mathbf{A}}$ and $\alpha_{\mathbf{C}}$ traces assuming that the relaxation time at T_g is approximately 100 s. Interestingly, the estimated steepness indices $m = -[\log \omega]/\mathrm{d}(T_g/T)|_{T=T_g}$ are seemingly quite different for both blocks. The **A** block shows the behavior of a fragile glass indicated by large $m_{\alpha,\mathrm{A}} \sim 136$ values while block index of $m_{\alpha,\mathbf{C}} \sim 48$ corresponding to values obtained for strong glasses. A reduction of m with side chain length has been also observed for other polymer series where internal plasticization appears like poly(*n*-alkyl methacrylates) containing alkyl groups with different length.[29] The β and γ processes of **A** and **C** block show the typical features of ordinary secondary relaxation processes related to localized motions. Their temperature dependence can be described by an Arrhenius law $\omega = \Omega \exp(-E_A/RT)$ with limiting frequencies Ω which are in both cases close to 10^{15} rad/s and activation energies which are $E_{A,\beta} = 21.4 \pm 3$ kJ/mol and $E_{A,\gamma} = 13.3 \pm 3$ kJ/mol for the β and γ processes, respectively. More unusual is the temperature dependence of the $\alpha_{\mathrm{fsc},\mathbf{C}}$ process. There are clear indications for a non-Arrhenius-like behavior although the $\alpha_{\mathrm{fsc},\mathbf{C}}$ trace appears linear in the Arrhenius plot in the accessible frequency window. An Arrhenius fit as shown in Figure 6 gives an apparent activation energy of about $E_{A,\mathrm{fsc}} = 68.8 \pm 6$ kJ/mol but a limiting frequency Ω of about 10^{35} rad/s. This value is an unphysical extrapolation since it is much higher than the upper frequency limit for relaxation processes of about 10^{14} rad/s. The indicates clearly that the $\alpha_{\mathrm{fsc},\mathbf{C}}$ relaxation frequencies must deviate from the discussed Arrhenius extrapolation, i.e., a non-Arrhenius-like temperature dependence must occur above our measurement window and the slope of the $\alpha_{\mathrm{fsc},\mathbf{C}}$ trace changes at high temperatures. The steepness index calculated from the trace of the $\alpha_{\mathrm{fsc},\mathbf{C}}$ process is $m_{\mathrm{fsc},\mathbf{C}} \sim 30$ corresponding to that of strong glasses. Similar behavior has been reported for the α_{PE} process in self-assembled alkyl nanodomains reported for various nanophase-separated side chain polymers containing long alkyl groups.[14,15] We conclude that the $\alpha_{\mathrm{fsc},\mathbf{C}}$ process shows indeed typical features of a dynamic glass transition and reflects most likely cooperative motions in nanodomains formed by aggregated side chains of the partly fluorinated **C** block with a typical size of about 2 nm.

4. Discussion

Hierarchy of Length Scales. The presented results show clearly that the investigated, $\mathbf{A}_m$-*b*-$\mathbf{C}_n$ block copolymers are self-assembled systems with a hierarchy of length scales in the nanometer range. Classical microphase separation of incompatible **A** and **C** blocks leads to a large scale structure with spacings of about 20−25 nm while nanophase separation of main and side chains in the **C** domains results in an internal structure with typical periodicities d_{nps} of about 2.9 nm. Like in side chain polymers containing long alkyl groups, nanophase separation of the **C** block with long partly fluorinated side chains is indicated by (i) a peak in the MAXS range at $q \sim 0.22$ Å^{-1} and (ii) a main chain independent dynamics in the side chain domains ($\alpha_{\mathrm{fsc},\mathbf{C}}$) showing a non-Arrhenius-like temperature dependence. Obviously, nanophase separation can also occur under confinement, i.e., in self-assembled **C** block domains which are only 10 times larger than d_{nps}.

The morphology of the investigated block copolymers with cylindrical ($\mathbf{A}_{50}$-*b*-$\mathbf{C}_{13}$) and lamellar ($\mathbf{A}_{50}$-*b*-$\mathbf{C}_8$) overall structure should be similar to that sketched in Figure 7. A similar overall structure has been proposed for other block copolymers containing comb-like blocks with long side chains in the amorphous, semicrystalline or liquid-crystalline state.[7−10,19] Note that the backbones of the **C** block are aligned basically perpendicular to the interfaces between both microphases and that the fluorinated side chains are noninterdigitated. Only under this condition one can explain the observed $d_{\mathrm{nps}} = 2.9$ nm values which are nearly twice larger than the extended length of the partly fluorinated side chains (1.4 nm) of the **C** block. Noninterdigitated side-chains have been also reported for comb-like homopolymers with partly fluorinated side chains[18−20] in contrast to the findings for many systems with alkyl side chains.[12,14,25,30] This might be reasonable considering the fact that in case of noninterdigitating semifluorinated side chains the contacts between alkylated and fluorinated units are minimized which should be energetically favorable.

Summarizing the discussed findings one can conclude that the two structure formation mechanisms in the investigated $\mathbf{A}_m$-*b*-$\mathbf{C}_n$ block copolymers can occur more or less independently. These copolymers can optimize seemingly their packing on two different length scales in parallel and form a structure-in-structure morphology. The competition between both structure formation mechanisms is obviously limited, i.e., side and mains chains of the comb-like block **C** can manage to nanophase separate like under bulk conditions. In some sense the situation seems to be different from that in microphase-separated block copolymers containing crystallizable components like polyethylene or poly(ethylene oxide).[31,32] In this case there is often a clear competition of both structure formation mechanisms, microphase separation and crystallization, since the thickness of the folded crystalline lamellae is typically similar to the size of the domains formed due to microphase separation (~10 nm).

Hence crystallization can destroy the original block copolymer morphology and strong nonequilibrium effects do appear.[33] The coexistence of two structure formation mechanisms which do not strongly compete like in our hierarchically structured block copolymers can be a useful strategy to design functional materials which are close to equilibrium but able to combine the properties of individual domains with different dimensions. Note that nanophase separated side chain polymers containing alkyl groups of different length are materials with truly predictable structure−property relations. Damping can be introduced in a controlled way since the frequency temperature position of the α_{PE} process in the alkyl nanodomains depends systematically on the side chains length (and nanodomain size d_{nps}) but basically not on the main chain properties.[12,15] Similar behavior would be expected for comb-like polymers in the nanophase-separated state containing other side chains, e.g., long partly fluorinated sequences. In combination with a systematic variation of the second block this can be used to fine-tune the mechanical properties of self-assembled systems with hierarchical structure. Other properties of such polymers might be optimized following the same strategy.

Early Stages of Nanophase Separation. An interesting finding of this work is that the peak in the MAXS range indicating a nanophase separation in phase **C** connected with an aggregation of long partly fluorinated side chains shows significant changes above 30 °C. The MAXS peak starts to broaden at this temperature during heating, disappears finally at temperatures around 90 °C but reappears during cooling. This observation can be interpreted as an indication for a transition from the nanophase-separated state to a disordered state without separation of main and side chains. Disappearance of the peak in the MAXS range at temperatures near 70 °C has been also reported for other polymeric systems which contain a component with partly fluorinated side chains.[34] Room-temperature ionic liquids being small molecules containing long alkyl tails show similar trends.[35] Comb-like polymers containing long alkyl groups, however, show usually a well pronounced scattering peak in the MAXS range until degradation starts to appear.[13] Hence systems with partly fluorinated side chains might be useful model systems to study the order-to-disorder transition (ODT) in nanophase-separated polymers. To have such model systems seems to be important since a theory which describes the behavior of nanophase-separated side chain polymers quantitatively is still missing. Information about the temperature dependence of the scattering intensity close to an order-to-disorder transition seems to be of special importance for the development of such theoretical models.

Although clear indications for an ODT belonging to the nanophase separation are seen in the data for our $\mathbf{A}_m$-*b*-$\mathbf{C}_n$ block copolymers, there are drawbacks preventing a detailed analysis. The problems have to do with the fact that the investigated systems are copolymers and only a certain fraction of the signal is coming from the comb-like **C** block which is undergoing nanophase separation. (i) The relatively broad MAXS peak in the scattering pattern at $q \sim 0.22$ Å^{-1} has a small intensity since only the **C** phase contributes. Moreover, nanophase and microphase separated structures coexist and the corresponding scattering peaks do partly superimpose. Both effects lead to a situation that makes it very complicated to analyze the temperature dependence of intensity and width of the MAXS peak seriously. (ii) Changes in the relaxation behavior, in particular the $\alpha_{fsc,C}$ process, near the speculated ODT would be also of major interest. Such changes could support the given interpretation since an independent dynamics within self-assembled side chain domains should disappear or change qualitatively above an ODT due to a transition to the disordered state without separated main and side chain domains and superstructure on the mesoscale. For the block copolymers studied in this work the $\alpha_{fsc,C}$ process is unfortunately inaccessible in dielectric spectra measured at the relevant temperatures (30−90 °C). Part of the evaluation problem are strong relaxation processes in the **A** block appearing at frequencies near the $\alpha_{fsc,C}$ process which hide the latter in the ε'' isotherms (Figure 5, parts c and e). A way out of this problem would be homopolymers of type **C**, which are unfortunately not producible yet due to solubility restrictions. Other comb-like polymers where semifluorinated side chains are attached to similar backbones might be an alternative.

Summarizing the discussion in this part we think that questions related to the nanophase separation behavior should be in the focus of further investigations on semifluorinated side chain polymers with a microstructure similar to that of the **C** block in our copolymers. One way to clarify details of their complex structure might be studies on oriented samples.[36] Further studies may contribute to a better understanding of the driving forces causing nanophase separation in side chain polymers which are still not finally clear. This could also help to make useful predictions about structure and properties of comb-like polymers based on the knowledge about their microstructure.

5. Conclusions

We have shown in this work that norbornene based block copolymers containing a comb-like component with semifluorinated side chains are systems which are hierarchically structured on the nanoscale. They show a structure-in-structure morphology since a microphase separation of both blocks (periodicity 20−25 nm) coexists with a nanophase separation of main and side chains in the phase formed by the comb-like component (periodicity ~3 nm). Although the length scales are not too different, both self-assembling mechanisms can occur. The energetic optimization of the systems seems to require both. The relaxation behavior of the investigated block copolymers is rather complex and incorporates a relaxation process (α_{fsc}) which is seemingly related to an independent dynamics in nanodomains formed by semifluorinated side chains with typical dimensions of about 2 nm. X-ray scattering data strongly indicate that the nanophase separation in the comb-like component disappears at temperatures between 30 and 90 °C. This finding for the semifluorinated block is interesting since polymeric systems showing that the nanophase separation of main and side chains disappears at accessible temperatures are not well investigated but important for a deeper understanding of the driving forces of such structure formation processes on extremely small length scales. Progress with a theoretical description of this phenomenon and microstructure-based predictions would be of importance for commercial users since comb-like polymers are used as functional materials in various fields of application.

Acknowledgment. The authors thank A. Petzold for assistance with the SAXS data analysis based on the interfacial distribution function. W.H.B. acknowledges grants from the DFG (INST 271/249-1, INST 271/247-1, and INST 271/248-1). M.B. thanks for financial support by the DFG (BE 2352/4-1) and the state Sachsen-Anhalt.

Supporting Information Available: Table of molecular weight (M_n) and PDI measured by GPC and figures showing GPC curves for homopolymer $\mathbf{A}_{50}$ and block copolymer $\mathbf{A}_{50}$-*b*-$\mathbf{C}_{13}$, ^{1}H and ^{13}C NMR spectra of monomers **A** and **C** and ^{1}H NMR spectrum of block copolymer $\mathbf{A}_{50}$-*b*-$\mathbf{C}_{13}$. This material is available free of charge via the Internet at http://pubs.acs.org.

References and Notes

(1) Hamley, I. W. *Nanotechnology* **2003**, *14*, R39.
(2) Bates, F. S.; Fredrickson, G. H. *Annu. Rev. Phys. Chem.* **1990**, *41*, 525.
(3) Hamley, I. W. *The physics of block copolymers*; Oxford University Press: Oxford, U.K., 1998.
(4) Muthukumar, M.; Ober, C. K.; Thomas, E. L. *Science* **1997**, *277*, 1225.
(5) Ikkala, O.; ten Brinke, G. *Science* **2002**, *295*, 2407.
(6) Ober, C. K.; Cheng, S. Z. D.; Hammond, P. T.; Muthukumar, M.; Reichmanis, E.; Wooley, K. L.; Lodge, T. P. *Macromolecules* **2009**, *42*, 465.
(7) Schneider, A.; Zanna, J.-J.; Yamada, M.; Finkelmann, H.; Thomann, R. *Macromolecules* **2000**, *33*, 649.
(8) Ansari, I. A.; Castelletto, V.; Mykhaylyk, T.; Hamley, I. W.; Lu, Z. B.; Itoh, T.; Imrie, C. T. *Macromolecules* **2003**, *36*, 8898.
(9) Hempel, E.; Budde, H.; Höring, S.; Beiner, M. *Lect. Notes Phys.* **2007**, *714*, 201.
(10) Gitsas, A.; Floudas, G.; Butt, H. J.; Pakula, T.; Matyjaszewski, K. *Macromolecules* **2010**, *43*, 2453.
(11) Chen, W.; Wunderlich, B. *Macromol. Chem. Phys.* **1999**, *200*, 283.
(12) Beiner, M. *Macromol. Rapid Commun.* **2001**, *22*, 869.
(13) Arbe, A.; Genix, A.-C.; Colmenero, J.; Richter, D.; Fouquet, P. *Soft Matter* **2008**, *4*, 1792.
(14) Beiner, M.; Huth, H. *Nat. Mater.* **2003**, *2*, 595.
(15) Pankaj, S.; Hempel, E.; Beiner, M. *Macromolecules* **2009**, *42*, 716.
(16) Stepanyan, R.; Subbotin, A.; Knaapila, M.; Ikkala, O.; ten Brinke, G. *Macromolecules* **2003**, *36*, 3758.
(17) Milner, S. T. *Macromolecules* **1994**, *27*, 2333.
(18) Honda, K.; Morita, M.; Otsuka, H.; Takahara, A. *Macromolecules* **2005**, *38*, 5699.
(19) Wang, J.; Mao, G.; Ober, C. K.; Kramer, E. J. *Macromolecules* **1997**, *30*, 1906.
(20) Kim, B. G.; Chung, J.-S.; Sohn, E.-H.; Kwak, S.-Y.; Lee, J.-C. *Macromolecules* **2009**, *42*, 3333.
(21) Neugebauer, D.; Theis, M.; Pakula, T.; Wegner, G.; Matyjaszewski, K. *Macromolecules* **2006**, *39*, 584.
(22) Binder, W. H.; Pulamagatta, B.; Kir, O.; Kurzhals, S.; Barqawi, H.; Tanner, S. *Macromolecules* **2009**, *41*, 8405.
(23) Adekunle, O.; Tanner, S.; Binder, W. H. *Beilstein J. Org. Chem.* **2010**, *6*, No. 59.
(24) Note that it is extremely hard to determine volume fractions in case of our block copolymers since homopolymer **C** has not been successfully synthesized yet. Hence its density is unknown and one can not use a combination of NMR data and density information to estimate volume fractions. We have tried to estimate the volume fractions for the $\mathbf{A}_{50}$-*b*-$\mathbf{C}_8$ sample with lamellar morphology based on the interfacial distribution function $K''(z)$. Assuming that **C** is the minority component one gets $\Phi_{\mathbf{C}} = 0.4-0.45$. As long the densities are identical one can estimate based on that information the volume fraction Φ_c for the $\mathbf{A}_{50}$-*b*-$\mathbf{C}_{13}$ sample. This gives values of about 0.5−0.62. $\Phi_{\mathbf{C}}$ values up to 0.7 seem to be possible for the $\mathbf{A}_{50}$-*b*-$\mathbf{C}_{13}$ sample considering an inverted phase situation in the lamellar sample $\mathbf{A}_{50}$-*b*-$\mathbf{C}_8$ what is not completely excluded in the light of the extended length of block **C**. Further experiments incorporating additional block copolymer samples are required to understand the situation in the phase diagram.
(25) Arrighi, V.; Triolo, A.; McEwen, I. J.; Holmes, P.; Triolo, R.; Amenitsch, H. *Macromolecules* **2000**, *33*, 4989.
(26) Heijboer, J. In *Physics of non crystalline solids*; Prins, J. A., Ed.; North Holland: Amsterdam, 1965; p 231.
(27) Floudas, G.; Antonietti, M.; Förster, S. *J. Chem. Phys.* **2000**, *113*, 3447.
(28) Beiner, M.; Korus, J.; Lockwenz, H.; Schröter, K.; Donth, E. *Macromolecules* **1996**, *29*, 5183.
(29) Floudas, G.; Stepanek, P. *Macromolecules* **1998**, *31*, 6951.
(30) Mierzwa, M.; Floudas, G.; Stepanek, P.; Wegner, G. *Phys. Rev. B* **2000**, *62*, 14012.
(31) Loo, Y.-L.; Register, R. A.; Ryan, A. J.; Dee, G. T. *Macromolecules* **2001**, *34*, 8968.
(32) Castillo, R. V.; Arnal, M. L.; Muller, A. J.; Hamley, I. W.; Castelletto, V.; Schmalz, H.; Abetz, V. *Macromolecules* **2008**, *41*, 879.
(33) Loo, Y.-L.; Register, R. A.; Ryan, A. J. *Macromolecules* **2002**, *35*, 2365.
(34) Al-Hussein, M.; Serero, Y.; Konovalov, O.; Mourran, A.; Moller, M.; de Jeu, W. H. *Macromolecules* **2005**, *38*, 9610.
(35) Triolo, A.; Russina, O.; Bleif, H.-J.; Di Cola, E. *J. Phys. Chem. B* **2007**, *111*, 4641.
(36) Clark, C. G.; Floudas, G. A.; Lee, Y. J.; Graf, R.; Spiess, H. W.; Müllen, K. *J. Am. Chem. Soc.* **2009**, *131*, 8537.